Urban Rail Transit
https://doi.org/10.1007/s40864-025-00260-w

http://www.urt.cn/

ORIGINAL RESEARCH PAPERS

The Decoupling Effect Analysis of Meteorological Comfort on Urban Rail Transit Ridership

Zhanwei Cui[1] · Yang Yang[2] · Shengye Hu[3] · Xin Liu[1] · Long Chen[4]

Received: 20 July 2025 / Revised: 27 October 2025 / Accepted: 3 November 2025

Abstract This study investigates the decoupling relationship between meteorological comfort and urban rail transit ridership in China. Daily meteorological data and passenger volume data from 28 major cities were processed to construct a meteorological comfort index using the entropy weighting method, in which precipitation levels were converted into continuous values based on national standards. A decoupling model was then applied to examine the dynamic interaction between weather comfort and transit use. The analysis identifies three classes of decoupling states: Class A, where passenger travel remains stable despite unfavorable weather; Class B, where moderate sensitivity to meteorological variation is observed; and Class C, where travel is strongly influenced by weather conditions. Results show that most cities predominantly fall under Class B, but with notable fluctuations across seasons and regions. The findings highlight that meteorological comfort does not uniformly determine ridership, but instead reveals differentiated patterns of resilience and vulnerability across urban rail systems. This contributes to a deeper understanding of how external environmental factors interact with public transit demand and provides methodological guidance for improving the robustness of transport planning under climate variability.

Keywords Urban rail transit ridership · Weather · Meteorological comfort · Decoupling

✉ Yang Yang
bjtuyang@bjtu.edu.cn; yangphd@buaa.edu.cn

Zhanwei Cui
swpolly@163.com

Shengye Hu
1581612971@qq.com

Xin Liu
liuxocean_539@126.com

Long Chen
chen0244@163.com

[1] Aerospace Era Low Altitude Technology Co., Ltd., Chongqing 404100, China

[2] School of Traffic and Transportation, Beijing Jiaotong University, Beijing 100044, China

[3] Tiangong University, Tianjin 300387, China

[4] Shijiazhuang Tiedao University, Hebei 050043, China

1 Introduction

The interdisciplinary study of meteorology and transportation has always been a very interesting topic, and almost all countries around the world are conducting studies in this area. For example, Toronto has conducted studies on the relationship between meteorology and rapid transit [1] and conventional transit [2]; Seoul, South Korea, has analyzed the change patterns of citizens choosing public transportation modes under different meteorological conditions [3]; and Qatar has analyzed the change patterns of meteorological conditions and public transportation volume in different seasons [4]. With the intensification of studies, many interesting conclusions have been drawn: the rainfall may reduce the demand for bicycles and buses, but may increase the demand for taxis [5]; when rainfall and low temperature are encountered on weekends, the passenger volume of public transportation will significantly decrease as compared to weekdays [6]. Nicole examined the effects of extreme weather events on bus ridership and the extent to which this relationship varies by income and destination [7]. In terms of the spatial variation, the operation of high-speed rail in the southeast coastal region was affected more frequently

Published online: 28 January 2026

by rain and thunderstorms, whereas the system operated in central–eastern China was more vulnerable to snowstorms [8].These study conclusions can explain the patterns of different meteorological conditions and choice of transportation modes, so as to help various cities better organize the operation when facing meteorological challenges.

Urban rail transit is one of the important components of urban transportation. However, meteorological changes may have adverse effects on the infrastructure of urban rail transit, thereby affecting operational efficiency and reliability, and potentially causing safety hazards. Understanding the impact of meteorological changes on urban rail transit can help develop more effective emergency plans and appropriate measures to reduce operational interruptions caused by meteorological changes, extend the service life of infrastructure, reduce the operating costs, and ensure the safety of passengers and employees. Therefore, studying the relationship between meteorological changes and urban rail transit can not only improve the safety and reliability of urban rail transit systems, but also optimize the operational management, reduce the negative impacts on the environment, improve the resilience of cities, and provide support for sustainable urban development.

In this paper, the impact of each single factor among maximum temperature, minimum temperature, precipitation, wind speed, and dressing index on the urban rail transit ridership is studied. In order to explore the relationship between the five factors and urban rail transit ridership, a meteorological comfort index model is firstly established based on the five factors, with the five factors grouped into one factor. Then, by establishing a decoupling evaluation model between passenger volume and meteorological comfort, the internal relationship between urban rail transit passenger volume and meteorological comfort is explained. Finally, through decoupling stability analysis, more rules were revealed, so as to further promote the progress of traffic management and meteorological study. This paper is organized into five parts: Literature Review, Theoretical Basis, Methods and Data, Results and Discussion, and Conclusions and Prospects.

2 Literature Review

Urban rail transit is an industry highly sensitive to meteorology [9]. The weather conditions such as strong wind, rainstorms, thunder, snow, and fog are likely to lead to failure of some equipment and facilities of trains, resulting in delay or even shutdown of trains and then causing panic among passengers [10]. Compared with sunny weather, 97% of urban rail transit stations show an increasing trend in daily average passenger volume under rainy and snowy weather conditions, which poses significant challenges to operational organization and management [11]. Extreme weather can cause serious interference to urban rail transit systems, leading to obvious economic, social and environmental consequences [12]. Using big data to analyze travel patterns in Washington, D.C., it is found that travel cost, natural environment, land use diversity, and network connectivity significantly affect the probability of individuals choosing taxis, shared bicycles, or rail transit [13]. In order to improve the comprehensive ability of urban rail transit to cope with different weather conditions, scholars have made many contributions in improving passenger service levels, mainly focusing on improving urban rail transit facilities and equipment, and studying the relationship between meteorology and urban rail transit passenger volume.

When studying how to improve and enhance the level of urban rail transit facilities and equipment, one direction is to study meteorology and urban rail transit stations. Common study directions also include studying how meteorology affects temperature changes within urban rail transit stations [14, 15], studying the connection situation of urban rail transit stations under different meteorological conditions [16] or willingness to choose travel modes [17], studying the impact of rainfall on passenger volume at different types of rail transit stations at different time periods throughout the day [18–20] and the sensitivity thereof [21], and studying the relationship between meteorological factors and stopping time of urban rail transit trains at stations [22].

The most common study direction is to study the relationship between meteorological types and urban rail transit passenger volume. The studies only involving one meteorological type mainly focus on rainfall [23, 24] or temperature [25]; the studies involving two meteorological types mainly focus on temperature and humidity [26], rainfall and snowfall [27], or rainfall and temperature [28]; the studies involving three meteorological types mainly focus on temperature, rainfall, and wind [29]; and the studies involving five meteorological types mainly focus on temperature, relative humidity, air pressure, wind speed, and rainfall [30]. The commonly used methods for studying the relationship between meteorological types and urban rail transit passenger volume include regression model [31], mixed logit model [32], and elastic model [33]. Usually, the change patterns of meteorological conditions and urban rail transit passenger volume are analyzed on an annual, quarterly and daily basis under the scenarios such as working days [34] and non-working days [35]. Timely meteorological warnings and sufficient emergency preparedness can effectively evacuate urban rail transit ridership, minimize the occurrence of urban rail transit accidents, minimize the damage to facilities, and improve the level of urban rail transit operation services [36]. Therefore, the prediction of meteorological conditions and urban rail transit passenger volume [37] is also one of the hot study topics. The commonly used data include meteorological data, urban rail transit passenger volume data, time data,

and location data, among which the meteorological data, time data, and location data are independent variables; the urban rail transit passenger volume data are dependent variable. The commonly used methods include the feature set simplification based on time series correlation and fuzzy means [38], the spatiotemporal loyalty prediction model [39], the real-time passenger volume-sensing meteorological system [40], the seasonal autoregressive comprehensive moving average prediction model [41], Multi-fusion residual network methods [42] and the deep learning neural network prediction model [43]. For deep learning neural network prediction model, the recurrent neural network (RNN) prediction model [44], the long short-term memory network (LSTM) prediction model [45, 46], or the combined prediction model based on these two models [47] may be adopted based on different independent variables. For the purpose of processing meteorological data, the feature value encoding method is often used [48]. The biggest advantage of this method is that it transforms string data into numbers, and thus is suitable for ordered data. However, its disadvantage is the poor interpretability. Xiu proposed a metro passenger flow prediction framework based on deep learning, combining correlation feature selection (Cor-STFS) and parallel spatiotemporal network (STA-PTCN-BIGRU) to improve prediction accuracy and computational efficiency [49]. Nian evaluated the subway line location based on network vulnerability, and optimized the new subway line planning of Pudong New Area by quantitatively analyzing the network performance under different interruption scenarios and adopting the tabu search algorithm, to improve operational reliability and resilience [50]. Optimizing the data sampling strategy can systematically evaluate the impact of bike-sharing data sample size on model estimation, inference and prediction [51].With the advent of the big data era, further study should be conducted on how to use big data to simultaneously consider historical passenger volume data and external meteorological factors [52], so as to comprehensively analyze the characteristics of urban rail transit passenger volume. At present, there are two approaches to study the travel behavior of urban rail transit. One focuses on the external environmental factors, such as the impact of meteorological comfort on rail transit passenger flow. The other focuses on the structural constraints of the built environment on commuting spatial behavior. The gradient boosting decision tree model is used to analyze the commuting behavior of low-income rental workers in Beijing. It is found that their commuting distance is nonlinearly affected by built environment factors such as public transport density, road density and land mix, and the commuting mode has a significant mediating effect [53]. Compared with the research focusing on the demand side of travel, some scholars have discussed how the built environment and technical engineering factors affect the supply structure of the rail transit system from the supply side of rail transit. Considering the five dimensions of geology and geomorphology, population coverage and earthquake risk, the multi-criteria decision-making method (MCDM) is used to realize the quantitative evaluation of route optimization [54]. This decision-making mechanism from the three-dimensional perspective of "space-engineering-serving population" provides another perspective of supply and demand for this paper to explore how meteorological comfort leads to the "decoupling effect" on the demand side. It shows that the track system itself contains structural constraints and selectivity in the construction stage.

In general, in the current studies on the impact of meteorology on urban rail transit travel, the focus is mainly placed on the impact of meteorological changes on rail transit as well as the and prediction thereof, and the urban rail transit passenger volume and various meteorological conditions are not evaluated and analyzed as a whole. The meteorological types still need to be improved, and the factors such as wind level, dressing index, and meteorological comfort indicators have not been taken into account. The fact that the meteorology in different regions varies at the same time has also not been taken into account. In terms of displaying daily urban rail transit passenger volume data, the scholars mentioned above mostly use bar charts and line charts for data display. There is a lack of exploration into data visualization when comparing and displaying the massive daily urban rail transit passenger volume data in different cities. Compared with existing studies, this research expands both the analytical dimension and methodological framework by integrating multiple meteorological indicators, adopting a decoupling perspective, and emphasizing multi-city comparative analysis. It is shown in Table 1.

In summary, prior research has made substantial progress in analyzing the relationship between meteorological factors and urban rail transit ridership. However, most studies have focused on single weather types, forecasting models, or supply-side infrastructure factors, while few have comprehensively evaluated the combined effect of multiple meteorological indicators through a comfort-based framework. In addition, issues such as variability in regional meteorology, daily-scale fluctuations, and novel visualization approaches remain underexplored. To address these gaps, this study constructs a meteorological comfort index integrating temperature, precipitation, wind speed, and dressing index, and applies a decoupling evaluation model to reveal differentiated resilience patterns in rail transit demand across 28 Chinese cities.

3 Theoretical basis

3.1 Supply and demand theory and urban rail transit

In economics, the relationship between supply and demand is usually used to describe the relationship between

Table 1 Comparison of previous studies and this study

Aspect	Previous studies	Limitations	This study
Research focus	Examined the impact of single or limited meteorological variables (e.g., rainfall, temperature, humidity) on rail transit ridership [23–30].	Most studies consider only one or two meteorological factors; lack of integrated comfort perspective.	Considers five meteorological dimensions (temperature, precipitation, wind level, dressing index, weather type) to build a comprehensive meteorological comfort index.
Data scope	Focused on individual cities (e.g., Beijing, Shanghai) or short-term samples [25, 31].	Lack of spatial comparison and long-term continuity.	Covers 28 cities across seven regions in China using daily data for 2023, enabling large-scale cross-regional analysis.
Analytical methods	Regression, Mixed Logit, elasticity, or deep learning prediction models [31–47].	Emphasized prediction, lacked interpretability and policy relevance.	Introduces decoupling analysis model to evaluate the dynamic relationship between meteorological comfort and ridership.
Data processing	Commonly used feature value encoding for categorical meteorological data [48].	Conversion accuracy limited; difficult to reflect real meteorological variability.	Uses Python-based stochastic transformation within official meteorological standards, preserving data randomness and realism.
Visualization	Mainly used bar and line charts [34, 35].	Limited ability to compare multi-city temporal variation.	Employs heatmap visualization for daily ridership, improving cross-city pattern recognition.
Research perspective	Focused mainly on external environmental effects.	Neglected the structural constraints of urban built environment.	Bridges meteorological (external) and urban structure (internal) perspectives through the decoupling framework.
Policy implications	Few direct implications for transport management.	//	Provides operational and scheduling insights for urban rail systems under varying meteorological conditions.

commodity prices and quantity demanded. In this study, this theoretical framework is extended to the context of urban rail transit. The passenger volume of urban rail transit is considered as demand, because it reflects the travel needs of passengers. Meteorological comfort is considered as supply, as it influences the service capacity of rail transit and constrains the effective realization of demand. When meteorological comfort deteriorates beyond a certain threshold, passenger demand for rail transit may stagnate or shift to other modes of transport as the supply approaches its operational limit. Therefore, it is essential to construct a model to examine the interaction between meteorological comfort and urban rail transit ridership.

3.2 Meteorological Comfort Index Model

A mathematical model is established based on the maximum temperature, minimum temperature, precipitation, wind speed, and dressing index. The calculation is shown in Eq. (1).

$$C = \gamma_1 P_{\text{Max-tem}} + \gamma_2 P_{\text{Min-tem}} + \gamma_3 P_{\text{pre}} + \gamma_4 P_{\text{wsp}} + \gamma_5 P_{\text{dco}} \quad (1)$$

where C is the meteorological comfort index; $\gamma_i, \quad i = 1, \ldots, 5$ are the weight coefficients, of which the calculation results are shown in Table 9; $P_{\text{Max-tem}}$ is the proportion of maximum temperature; $P_{\text{Min-tem}}$ is the proportion of minimum temperature; P_{pre} is the proportion of precipitation; P_{wsp} is the proportion of wind speed; and P_{dco} is the proportion of dressing index. The calculation of weight coefficients and proportions can be found in Step 3 as specified in 3.7 "Calculation Steps," namely using the entropy method to calculate the meteorological comfort index.

The dressing index is a model established on the basis of maximum temperature, minimum temperature, wind speed, solar constant, human metabolic rate, and latitude of city. This model improves the model proposed by Freitas C in 1979 [55], with the main improvement being changing the maximum temperature from 33 °C to the maximum temperature within the statistical range. This is because that, with global warming, the temperature is also increasing [56], and still using 33 °C as the maximum temperature will result in a negative dressing index, which is obviously incorrect. This model also takes into account the different characteristics of meteorology affected by terrain characteristics, as expressed in Eq. (2). The constants (0.155, 0.62, and 19.2) follow the empirical parameters established in the Freitas (1979) model, which quantify the balance between air temperature, wind velocity, and human thermal regulation, and have been retained to ensure methodological consistency and comparability.

$$Q_{\text{dco}} = \frac{T_{\max} - T_{\text{ave}}}{0.155H} - \frac{H + \alpha R \cos\alpha}{\left(0.62 + 19.2\sqrt{v}\right)H} \quad (2)$$

Q_{dco} is the dressing index; $T_{\max}$ is the maximum temperature occurring in the previous year in the place under study; T_{ave} is the average daily temperature, namely the average of the sum of the maximum and lowest temperatures in a day; H is 75% of the human metabolic rate, which is set as 87 W/m^2; R is the solar constant, namely 1357 W/m^2; α is the solar altitude angle, the latitude of the place under study is β, the specific values are shown in Table 1, the solar altitude angle α during spring and autumn is $90° - \beta$, the α during summer is $90° - \beta + 23°26'$, and the α during winter is $90° - \beta - 23°26'$; and v is the daily wind speed, expressed in m/s.

3.3 Passenger Volume–Meteorological Comfort Decoupling Evaluation Model

In order to more accurately describe the relationship between passenger volume increase and environmental degradation, a decoupling evaluation model for passenger volume and meteorological comfort is established. Due to the fact that the meteorological comfort is established based on five factors (namely maximum temperature, minimum temperature, precipitation, wind speed, and clothing index), the meteorological comfort index can be used as an indicator of environmental impact, and can also be used to comprehensively analyze the relationship between urban rail transit passenger volume and such five factors. The calculation formula for this model is shown in Eq. (3).

$$\text{DI} = \frac{(Q_s - Q_{s-1})/Q_{s-1}}{(C_s - C_{s-1})/C_{s-1}} = \frac{\Delta Q/Q_{s-1}}{\Delta C/C_{s-1}} \quad (3)$$

Q is the daily rail transit passenger volume of the place under study; s is the date; DI is the decoupling index, of which the judgment rules are shown in Table 2; ΔQ is the increase rate of urban rail transit passenger volume; ΔC is the increase rate of meteorological comfort index, and if $\Delta C > 0$, it can be understood as environmental degradation. s denotes the observation period (day). Since the calculation requires both period s and $s-1$, the minimum value of s is 2, corresponding to the second observation day.

The judgment rules for decoupling are interpreted as follows:

"Expansion-based negative decoupling" refers to the situation that the urban rail transit passenger volume increases under environmental degradation, with the increase rate of urban rail transit passenger volume being greater than the increase rate of meteorological comfort index.

Table 2 Rule of decoupling

Evaluation	Decoupling State	DI	ΔQ	ΔC
A	Expansion-based negative decoupling	DI > 1.2	$\Delta Q > 0$	$\Delta C > 0$
B	Strong negative decoupling	DI < 0	$\Delta Q > 0$	$\Delta C < 0$
B	Expansion-based coupling	$0 \le$ DI ≤ 1.2	$\Delta Q \ge 0$	$\Delta C > 0$
C	Decline-based decoupling	DI > 1.2	$\Delta Q < 0$	$\Delta C < 0$
C	Weak negative decoupling	$0 \le$ DI ≤ 1.2	$\Delta Q \le 0$	$\Delta C < 0$
C	Strong decoupling	DI < 0	$\Delta Q < 0$	$\Delta C > 0$

"Strong negative decoupling" refers to the situation that urban rail transit ridership increases when the meteorological comfort index decreases.

"Expansion-based coupling" refers to the situation that the urban rail transit passenger volume increases under environmental degradation, with the increase rate of urban rail transit passenger volume being smaller than the increase rate of meteorological comfort index.

"Decline-based decoupling" refers to the situation that the urban rail transit passenger volume decreases when the meteorological comfort index decreases, but the increase rate (negative value) of passenger volume is smaller than the increase rate (negative value) of meteorological comfort index.

"Weak negative decoupling" refers to the situation that the urban rail transit passenger volume decreases when the meteorological comfort index decreases, but the increase rate (negative value) of passenger volume is greater than the increase rate (negative value) of meteorological comfort index.

"Strong decoupling" refers to the situation that the urban rail transit passenger volume decreases under environmental degradation.

Class A is the most ideal state, representing that people's travel is not affected by environmental degradation; Class B represents that people's travel can resist limited environmental degradation; Class C represents that people's travel is affected by the environment to a relatively large extent.

3.4 Passenger Volume–Meteorological Comfort Decoupling Stability Model

The passenger volume–meteorological comfort decoupling situation varies in each city, so that it is necessary to analyze the stability of passenger volume–meteorological comfort decoupling in each city. Regarding the indicator of decoupling stability, a passenger volume–meteorological comfort decoupling stability indicator is constituted by reference to the method proposed by Qi Jing[57], as shown in Eq. (4).

$$\delta = \frac{1}{I-1}\sum_{s=2}^{I}\left|\frac{\mathrm{DI}_s - \mathrm{DI}_{s-1}}{\mathrm{DI}_{s-1}}\right| \tag{4}$$

I is the total study time, DI_s is the decoupling index on the date s, the lower value of δ indicates the more stable decoupling state, and the higher value indicates the more unstable decoupling state.

4 Methods and Data

4.1 Study Assumptions and Data Resources

In the study, the following assumptions are made: (1) The passengers voluntarily choose rail transit as their travel mode. (2) There is no decrease in the availability of rail transit and other transportation modes, provided that the suspension of a mode for no more than 24 hours does not count as a decrease in availability.

The data used in this study are as follows: (1) Passenger volume data from rail transit systems in 28 cities, which, according to the first-level regional division of land meteorological geography in China, are classified into North China region, including three cities (namely Beijing, Tianjin, and Shijiazhuang), northeast region, including four cities (namely Shenyang, Harbin, Dalian, and Changchun), East China region, including eight cities (namely Shanghai, Nanjing, Suzhou, Qingdao, Hefei, Nanchang, Xiamen, and Changzhou), Central China region, including three cities (namely Wuhan, Changsha, and Zhengzhou), South China region, including five cities (namely Guangzhou, Shenzhen, Nanning, Foshan, and Dongguan), southwestern region, including four cities (namely Chengdu, Chongqing, Kunming, and Guiyang), and northwest region, including one city (namely Xi'an); the latitude data of each city is shown in Table 3. (2) Meteorological Data: The daily maximum temperature, minimum temperature, weather, wind direction, and date in 2023 in study cities were obtained using Python on the "Weather+" website (https://lishi.tianqi.com/); the data types and samples are shown in Table 4. Specifically, the meteorological data collection was carried out between

Table 3 City classification and latitude data sheet

City	Latitude	Region	City	Latitude	Region	City	Latitude	Region	City	Latitude	Region
Harbin	45.54774	Northeast region	Qingdao	36.30744	East China region	Xiamen	24.48405	East China region	Wuhan	30.58203	Central China region
Changchun	43.83327	Northeast region	Hefei	31.79322	East China region	Guangzhou	23.15792	South China region	Changsha	28.25591	Central China region
Shenyang	41.80515	Northeast region	Changzhou	31.72322	East China region	Dongguan	23.02067	South China region	Xi'an	34.23053	Northwest region
Dalian	38.95223	Northeast region	Shanghai	31.40527	East China region	Foshan	22.90026	South China region	Chengdu	30.65984	Southwest region
Beijing	40.22077	North China region	Nanjing	31.32751	East China region	Nanning	22.78121	South China region	Chongqing	29.40268	Southwest region
Tianjin	39.71755	North China region	Suzhou	31.30227	East China region	Shenzhen	22.55329	South China region	Guiyang	26.67865	Southwest region
Shijiazhuang	38.03647	North China region	Nanchang	28.54538	East China region	Zhengzhou	34.72468	Central China region	Kunming	24.88554	Southwest region

February and March 2024 using a Python-based crawler script (Python 3.9, requests 2.28, BeautifulSoup 4.11), ensuring complete coverage of all daily records for 2023. (3) Date Data: Distinguished by national public holidays in 2023, where "non-working days" refer to Saturdays and Sundays (excluding those designated as statutory compensatory leave) and public holidays (including New Year's Day, Spring Festival, Tomb Sweeping Day, Labor Day, Loong Boat Festival, Mid-Autumn Festival and National Day) in 2023; working days refer to the days other than non-working days. The definition and classification of working days and non-working days in 2023 are shown in Table 5. (4) Special Events. In response to complex and ever-changing meteorological conditions, from the perspective of ensuring personal and property safety, Beijing, Guangzhou, Shenzhen, Foshan, Dongguan and Xiamen have all taken measures to interrupt the operation of urban rail transit; from the perspective of encouraging citizens to choose public transportation to alleviate the impact of meteorological deterioration, Shijiazhuang has taken measures to encourage travel. The measures taken by various cities and the timing thereof are shown in Table 6.

4.2 Principle and Analysis of Heatmap

To visualize the large-scale passenger volume matrix across 28 cities, this study adopts the heatmap approach, which has been widely used in transportation and environmental studies for pattern recognition and anomaly detection [58].

In this study, to avoid data concentration in the allocation of color for the heatmap caused by different orders of magnitude of urban rail transit passenger volume, the range normalization method is adopted for the daily rail transit passenger volume of each city in 2023, as shown in Eq. (5). Firstly, the data normalization is carried out, and then, a heatmap of daily urban rail transit passenger volume is established. Due to the use of the range method for data normalization, the data of different orders of magnitude can be normalized, so as to effectively compare them; however, the disadvantage is that, for a certain city, the maximum passenger volume may increase sharply due to special policies, which will affect the distribution of data for that city.

4.3 Entropy Method and Correlation Coefficient Analysis

The entropy method, widely used in multi-indicator evaluation, objectively determines indicator weights based on their information entropy and variability [59]. In this study, it is employed to evaluate the relative contribution of maximum temperature, minimum temperature, wind speed, precipitation, and dressing index to meteorological comfort.

Table 4 Meteorological data types and samples

Type	City	Maximum temperature	Minimum temperature	Weather	Wind direction	Date
Data Type	Text	Text	Text	Text	Text	Text
Sample Data	Shanghai	17 °C	9 °C	Moderate rain	Northeast wind level 1	Friday, January 13, 2023

Table 5 Definition and scope of 2023 working days and non-working days

Type	Non-working days		Working days
Meaning	Regular rest days and national public holidays		Days other than non-working days
Scope	Saturday	Excluding those designated as compensatory working day	Including regular Monday, Tuesday, Wednesday, Thursday, and Friday, as well as compensatory working days as stipulated in the *Labor Law of the People's Republic of China*
	Sunday	Excluding those designated as compensatory working day	
	New year's day	January 1–2	
	Spring festival	January 21–27	
	Tomb sweeping day	April 5	
	Labor day	April 29–May 3	
	Loong boat festival	June 22–24	
	Mid-autumn festival and national day	September 29–October 6	
Days	A total of 115 days		A total of 250 days

Table 6 Special events in 2023

City	Type of measure	Special event
Shijiazhuang	Measures to encourage travel	From December 16 to December 31, 2023, Shijiazhuang began implementing free subway and bus activities, so as to cope with the complex and changing weather conditions and facilitate citizens to choose public transportation for travel.
Beijing	Operation interruption measures	From July 30 to 31, 2023, due to the impact of rainstorm, Beijing Urban Rail Transit Line 2 implemented the measures such as closure and nonstop passage, with 5 key lines extending their operating hours; 175 bus/tram lines took measures such as stopping, interval measures, bypassing stations, and connecting at night.
Guangzhou	Operation interruption measures	From 19:00 on September 1, 2023 to 08:33 on September 2, 2023, some urban rail transit lines and bus/tram lines in Guangzhou were partially suspended due to the impact of Typhoon "Saola."
Shenzhen	Operation interruption measures	From 19:00 on September 1, 2023 to 08:33 on September 2, 2023, some urban rail transit lines and bus/tram lines in Shenzhen were partially suspended due to the impact of Typhoon "Saola."
Foshan	Operation interruption measures	From 22:30 on September 1, 2023 to 11:00 on September 2, 2023, some urban rail transit lines and bus/tram lines in Foshan were partially suspended due to the impact of Typhoon "Saola."
Dongguan	Operation interruption measures	From 20:00 on September 1, 2023 to 08:00 on September 2, 2023, some urban rail transit lines and bus/tram lines in Dongguan were partially suspended due to the impact of Typhoon "Saola."
Xiamen	Operation interruption measures	From 20:00 on July 27, 2023 to 15:00 on July 28, 2023, Xiamen implemented the "three suspensions and one rest" policy due to the impact of Super Yyphoon "Doksuri," with the public transportation such as urban rail transit, BRT, and bus/tram suspended.

The Pearson correlation coefficient is a classical statistical measure of linear association between two variables [60]. Here, it is applied to assess the correlation between meteorological indicators and urban rail transit ridership in each city, with scatter plots illustrating the sign and strength of these relationships.

4.4 Calculation Steps

There are a total of six calculation steps, which are detailed as follows.

Step 1 is processing the data. The textual data are converted into numerical data by using Python as the tool. The maximum temperature, minimum temperature, and date are extracted by segmenting characters and extracting numbers, while the wind direction is extracted by segmenting characters, extracting the last two characters and placing the extracted content into "wind level." The textual data about weather and wind level are converted into numerical data in accordance with the classification standards for precipitation (snowfall) intensity level (see Table 7) and the classification standards for wind power level (see Table 8) issued by the National Meteorological Administration. This is because the snowfall level standard usually refers to the standard for converting continuous snowfall or snowfall amount into precipitation amount within a specified time period, so that snowy days can be converted into precipitation amount. Python is used to randomly generate numbers within the corresponding level range, where the classification standard for precipitation (snowfall) intensity level adopts the 12-hour interval with the total precipitation amount (mm) being a random number, and the wind speed is the wind speed at a standard height of 10m on open flat ground. After data preprocessing, the textual weather is transformed into precipitation amount,

Table 7 Classification standard of precipitation (Snowfall) intensity

Item	Total precipitation in 12 hours (mm)	Item	Total precipitation in 12 hours (mm)
Sporadic rain	<0.1	Light snow	<0.1
Light rainfall	0.1~4.9	Moderate snow	0.1~0.9
Moderate rain	5.0~14.9	Major Snow	1.0~2.9
Heavy rain	15.0~29.9	Blizzard	3.0~5.9
Torrential rain	30.0~69.9	Great blizzard	6.0~9.9
Downpour	70.0~139.9	Extremely great blizzard	10.0~14.9
Heavy downpour	≥140.0	Extremely heavy rainstorm	> 15.0

Table 8 Classification standard of wind

Wind level	Name	Wind speed (m/s)	Wind level	Name	Wind speed (m/s)
0	Windless	0–0.2	7	High wind	13.9–17.1
1	Soft wind	0.3–1.5	8	Gale	17.2–20.7
2	Gentle breeze	1.6–3.3	9	Great gale	20.8–24.4
3	Breeze	3.4–5.4	10	Fierce gale	24.5–28.4
4	Gentle wind	5.5–7.9	11	Storm	28.5–32.6
5	Strong wind	8.0–10.7	12	Hurricane	32.7–36.9
6	Heavy wind	10.8–13.8	13	–	37.0–41.4

Table 9 Results of sample data preprocessing

Type	City	Maximum temperature	Minimum temperature	Weather	Wind direction	Date
Data type	Text	Text	Text	Text	Text	Text
Sample data	Shanghai	17 °C	9 °C	Moderate rain	Northeast wind level 1	Friday, January 13, 2023
The preprocessing of data is carried out, where the weather is ultimately represented by precipitation amount and the wind direction is ultimately represented by wind speed						
Data type (after processing)	Text	Number	Number	Number	Number	Date
Sample data (after processing)	Shanghai	17	9	12.73	1.43	January 13, 2023

and the wind direction is transformed into wind speed. The results of sample data conversion are shown in Table 9. All parameter values in this model are determined according to the official classification standards of the China Meteorological Administration. When applying the model to other countries or regions, the corresponding local meteorological classification standards and climatic conditions should be adopted to ensure validity.

As the available datasets contain only categorical descriptions, rather than precise millimeter values, a random sampling approach is used to convert precipitation levels to continuous numerical values. Specifically, for each day, a random number is generated within the range of standard values at the corresponding classification level. There are two reasons for this decision. First, it preserves the natural randomness of weather conditions, which better reflects real-world variability than a fixed average. Second, the core purpose of this study is to analyze the decoupling effect between meteorological comfort and traffic travel on a daily basis, where it is crucial to capture subtle fluctuations. Using averages will artificially smooth the weather comfort index and may underestimate the actual environmental changes that influence behavior. At the same time, under the condition of the same weather before and after the encounter, the use of the average value will cause the same meteorological comfort index, which will cause the denominator of the passenger volume–meteorological comfort decoupling evaluation model to be zero, so that the model cannot operate normally. The calculations were carried out in the passenger volume–meteorological comfort decoupling stability model with random numbers and average values. It is found that the results of average values are far greater than those of random numbers, which also proves the above statement. The calculation results are shown in Table 11.

Step 2 is calculating the dressing index. According to Eq. (2), the daily dressing index is calculated.

Step 3 is using the entropy method to calculate the meteorological comfort index. Using the entropy method, the meteorological comfort index is calculated according to Eq. (1). The specific steps are as follows:

Step 3-1: Using the range normalization method to normalize the original data set, so as to eliminate the dimensional differences in each indicator, and compress the value of each indicator within the range of [0,1]. Assuming that the original data matrix X is composed of m samples and n indicators, namely $X = (X_{i,j})_{m*n}$, then the calculation of range standardization is shown in Eq. (5).

$$X_{i,j}^{1} = \frac{X_{i,j} - \min(X_{1,j}, X_{2,j}, \ldots, X_{m,j})}{\max(X_{1,j}, X_{2,j}, \ldots, X_{m,j}) - \min(X_{1,j}, X_{2,j}, \ldots, X_{m,j})} \quad (5)$$

$X_{i,j}^{1}$ is the range-standardized data; i is the sample i; j is the indicator j; and m is the number of samples. In this study, when calculating the meteorological comfort, $m = 365$; n is the number of indicators, and is set as $n = 5$, indicating maximum temperature, minimum temperature, precipitation, wind speed, and dressing index. When handling the range normalization of urban rail transit passenger volume, $m = 365$; n is the number of cities, and is set as $n = 28$, indicating Shanghai, Beijing, Guangzhou, Shenzhen, Chengdu, Wuhan, Chongqing, Xi'an, Nanjing, Changsha, Zhengzhou, Tianjin, Suzhou, Shenyang, Qingdao, Hefei, Nanchang, Nanning, Kunming, Harbin, Xiamen, Dalian, Changchun, Shijiazhuang, Guiyang, Changzhou, Foshan, and Dongguan.

Step 3-2: Calculating the value proportion of the sample i of the indicator j, with the calculation formula shown in Eq. (6).

$$P_{ij} = \frac{X_{ij}^{1}}{\sum_{i=1}^{m} X_{ij}^{1}}, \quad i = 1, \ldots, m, \quad j = 1, \ldots, n. \quad (6)$$

P_{ij} is the value proportion of the sample i of the indicator j.

Step 3-3: Calculating the weight γ_j of the indicator j, with the calculation formula shown in Eq. (7).

$$\gamma_j = \frac{1 + (\frac{1}{\ln m} \sum_{i=1}^{m} P_{ij} \ln P_{ij})}{\sum_{i=1}^{n} \left[1 + \left(\frac{1}{\ln m} \sum_{i=1}^{m} P_{ij} \ln P_{ij}\right)\right]} \quad (7)$$

γ_j is the weight coefficient.

Step 4 is calculating the passenger volume–meteorological comfort decoupling evaluation model and stability model, and then carrying out analysis and discussion.

The pseudocode for meteorological data preprocessing and comfort index calculation is as follows.

Algorithm 1 Meteorological data preprocessing and comfort index calculation

Input: Raw daily meteorological text data (temperature, weather, wind), 365 days

Output: Normalized meteorological comfort index for each day

1. Initialize empty arrays:

$$MaxTemp[\ ],\ \mathrm{MinTemp}[\ ], Precipitation[\ ], WindSpeed[\ ], DressIndex[\ ]$$

2. FOR each day in dataset:
   a. Extract maximum temperature and minimum temperature from text
   b. Extract wind direction; convert to numerical wind speed using national standard (Table 8)
   c. Identify weather description (e.g., “light rain”, “moderate snow”)
   d. Convert weather description into numeric precipitation:
      IF using random method:
         Generate a random value within the standard range of the level (see Table 7)
      ELSE IF using midpoint method (for robustness test):
         Use midpoint of corresponding level
   e. Store extracted values into arrays

3. Compute daily dressing index using Formula (2); store in $DressIndex[\ ]$

4. Form the raw data matrix X with $m = 365$ rows (days) and $n = 5$ columns:

$$X = [MaxTemp,\ MinTemp,\ Precipitation,\ WindSpeed,\ DressIndex]$$

5. Normalize X using range normalization (Formula 5):

   FOR each column j in X :

      Compute $\min(X[:, j])$ and $\max(X[:, j])$

      FOR each row i :

$$X\_norm[i][j] = (X[i][j] - \min\_j) / (\max\_j - \min\_j)$$

6. Compute proportion matrix P using Formula (6):
   FOR each j in columns:

$$col\_sum = sum(X\_norm[:, j])$$

      FOR each i :

$$P[i][j] = X\_norm[i][j] / col\_sum$$

7. Compute entropy weights γ_j using Formula (7):
   FOR each indicator j :

$$e\_j = -(1/\ln(m)) * sum(P[i][j] * \ln(P[i][j]))$$

$$\gamma\_j = (1 - e\_j) / sum(1 - e\_j) \text{ over all } j$$

8. Compute daily meteorological comfort index:
   FOR each day i :

$$ComfortIndex[i] = sum(P[i][j] * \gamma\_j \text{ for } j = 1 \text{ to } 5)$$

Return: $ComfortIndex[\ ]$

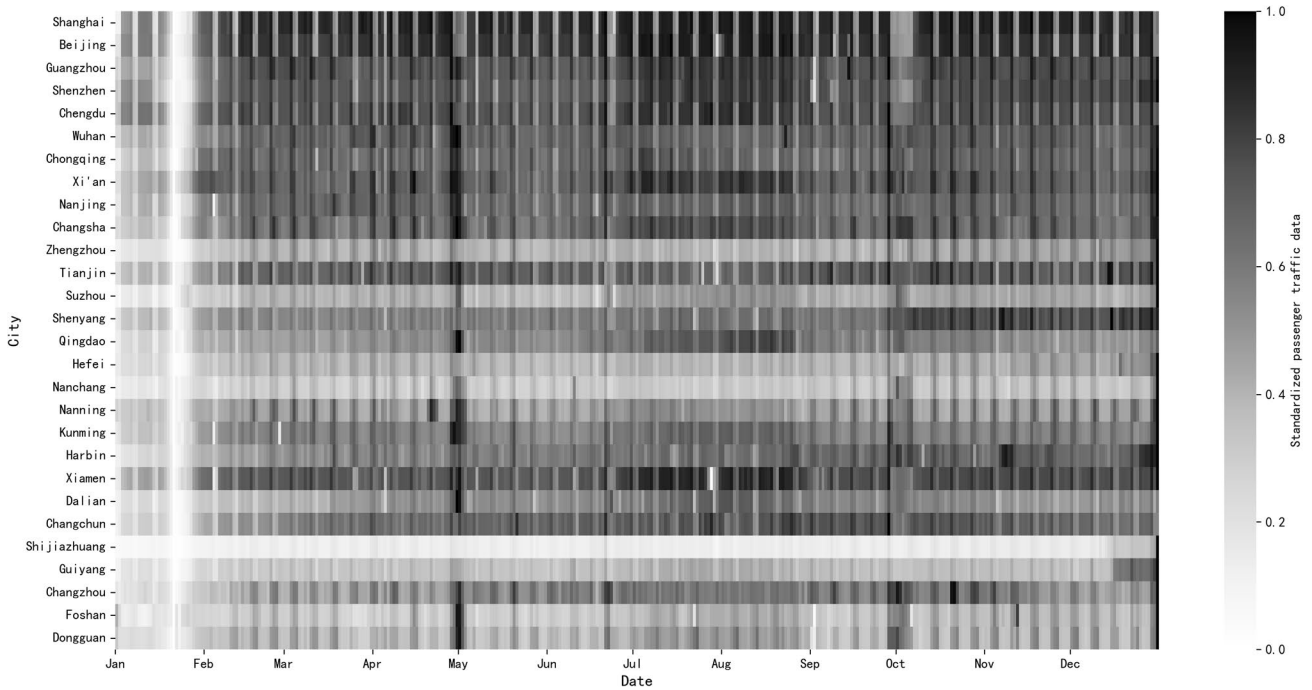

Fig. 1 Daily distribution of urban rail transit ridership in different cities

5 Results and Discussion

5.1 Analysis on Daily Travel Differences in Urban Rail Transit

In this section, the daily urban rail transit passenger volume of 28 cities in 2023 is visualized using a heatmap, with daily dates as the horizontal axis and cities ranked by annual passenger volume as the vertical axis.

As shown in Fig. 1, all cities except Shijiazhuang exhibit clear weekday/non-weekday patterns, reflecting differences in passenger volume between working and non-working days. In most cities, weekday ridership is higher, while in nine cities (e.g., Dongguan, Foshan, Changzhou, Nanning) non-working day ridership exceeds weekday levels. Shijiazhuang shows no obvious pattern due to special travel encouragement measures implemented on December 16, which gradually boosted ridership. Meteorological disruptions also led to temporary suspensions in six cities (e.g., Beijing, Guangzhou, Shenzhen), where passenger volumes dropped markedly.

Seasonal and holiday effects are also apparent. During the Spring Festival, passenger volume across all 28 cities reached its annual minimum, reflecting both family gatherings and the large-scale holiday migration. Conversely, during the Labor Day holiday, 12 tourist cities (e.g., Wuhan, Chongqing, Xi'an, Nanjing) recorded their annual peak ridership, while Shanghai and Beijing showed relatively lower demand. These findings highlight the strong influence of holidays and special events on ridership and suggest that cities should adjust train schedules accordingly—reducing services in low-demand periods and enhancing capacity during peaks.

5.2 Impact of Meteorological Factors on Meteorological Comfort Index

In this section, the meteorological comfort index is discussed, along with the weights assigned to maximum temperature, minimum temperature, wind speed, precipitation, and clothing index. According to Fig. 2 and Table 10, precipitation has the greatest contribution to the comprehensive evaluation of meteorological comfort index among all cities. The city with the highest weight (0.06) for maximum temperature is Zhengzhou, and the city with the lowest weight (0.02) for maximum temperature is Kunming; the city with the highest weight (0.06) for minimum temperature is Xi'an, and the city with the lowest weight (0.03) for minimum temperature is Shenzhen; the city with the highest weight (0.82) for precipitation is Shijiazhuang, and the city with the lowest weight (0.68) for precipitation is Guiyang; the city with the highest weight (0.15) for wind speed is Chongqing, and the city with the lowest weight (0.06) for wind speed is Shijiazhuang; the city with the highest weight (0.11) for dressing index is Nanning, and the city with the lowest weight (0.05) for dressing index is Shijiazhuang.

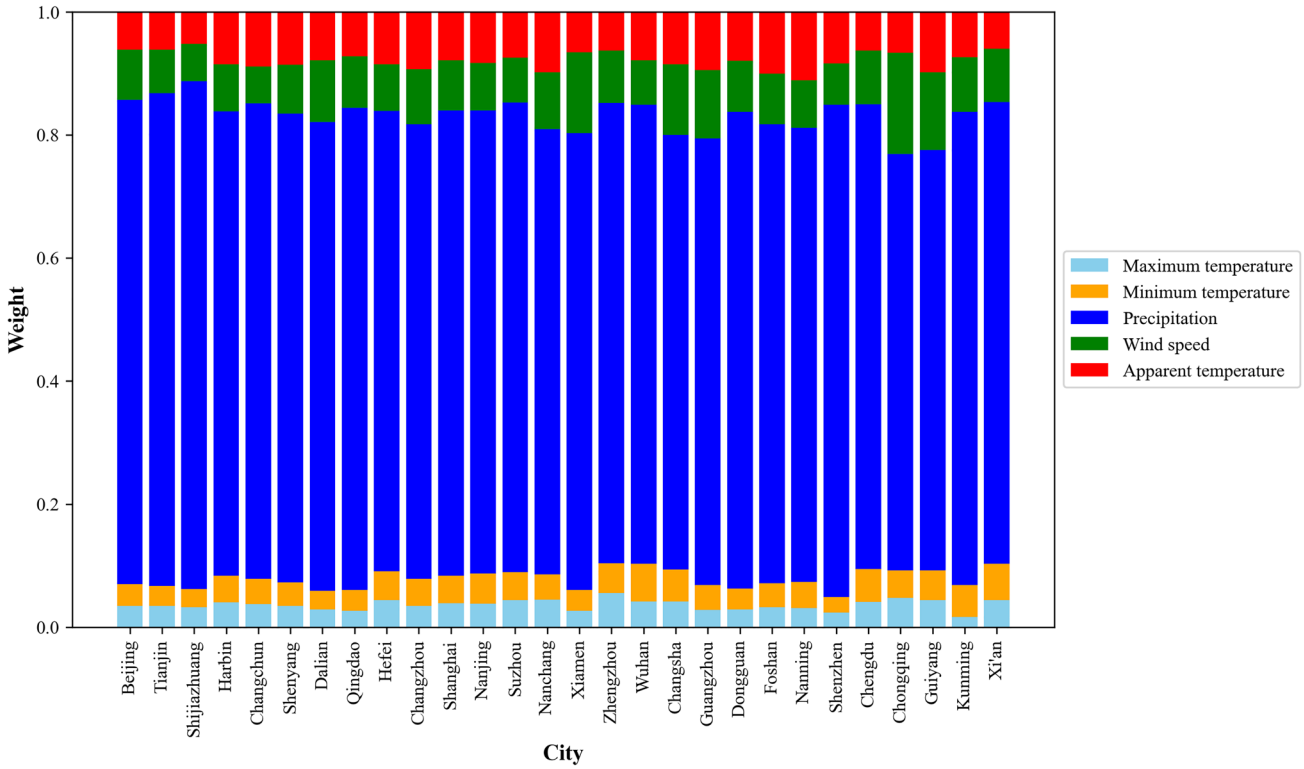

Fig. 2 Weight coefficient distribution of each factor in meteorological comfort index

The weight of the factors maximum temperature, minimum temperature, wind speed, precipitation, and dressing index in the meteorological comfort index varies in each city, which also verifies that the meteorology exhibits different characteristics in different regions, and indicates that it is necessary to conduct analysis between different regions when comprehensively analyzing the relationship between various meteorological factors and urban rail transit passenger volume.

5.3 Impact of Meteorological Factors on Urban Rail Transit Travel

In this section, the data from 28 cities are used to calculate the Pearson correlation coefficient between daily maximum temperature, minimum temperature, wind speed, precipitation, or dressing index, and passenger volume in each city, in order to explore the relationship between individual meteorological factors and urban rail transit passenger volume.e

The cities are classified according to the first-level regional division of land meteorological geography in China, the cities in each region are sorted in descending order of latitude, and a scatter plot of the Pearson correlation coefficient calculation results is made, as shown in Fig. 3. It can be found that the city most affected by maximum temperature is Qingdao, and the city least affected by maximum temperature is Shenyang; only Shijiazhuang is negatively correlated, while all other cities are positively correlated. The city most affected by minimum temperature is Qingdao, and the city least affected by minimum temperature is Zhengzhou; only Shijiazhuang is negatively correlated, while all other cities are positively correlated. The city most affected by wind speed is Harbin, and the city least affected by wind speed is Shanghai; only Dalian, Wuhan, Chongqing, Shijiazhuang, and Qingdao are negatively correlated, while all other cities are positively correlated. The city most affected by precipitation is Xiamen, and the city least affected by precipitation is Harbin; only Chongqing, Kunming, Changchun, Qingdao, Chengdu, Guiyang, Shanghai, Suzhou, and Harbin are positively correlated, while all other cities are negatively correlated. The city most affected by dressing index is Qingdao, and the city least affected by dressing index is Hefei; only Shijiazhuang is positively correlated, while all other cities are negatively correlated.

In the North China region, the maximum temperature, minimum temperature, and wind speed decrease as the latitude of city decreases, there is no significant relationship between precipitation/dressing index and latitude of city, and the precipitation is concentrated around −0.06. In the Northeast region, these five factors are not significantly related to

Table 10 Weight coefficient of each factor in meteorological comfort index

City	Maximum temperature	Minimum temperature	Precipitation	Wind speed	Dressing index	City	Maximum temperature	Minimum temperature	Precipitation	Wind speed	Dressing index
Beijing	0.03	0.03	0.80	0.08	0.06	Xiamen	0.03	0.03	0.75	0.12	0.07
Tianjin	0.03	0.03	0.82	0.06	0.06	Zhegnzhou	0.06	0.05	0.75	0.08	0.07
Shijiazhuang	0.03	0.03	0.82	0.06	0.05	Wuhan	0.04	0.06	0.76	0.07	0.08
Harbin	0.04	0.05	0.74	0.08	0.09	Changsha	0.04	0.05	0.70	0.12	0.08
Changchun	0.04	0.05	0.75	0.06	0.10	Guangzhou	0.03	0.04	0.75	0.10	0.09
Shenyang	0.03	0.04	0.76	0.09	0.09	Dongguan	0.03	0.04	0.76	0.09	0.09
Dalian	0.03	0.03	0.78	0.10	0.07	Foshan	0.03	0.04	0.76	0.07	0.10
Qingdao	0.03	0.03	0.79	0.08	0.07	Nanning	0.03	0.04	0.73	0.08	0.11
Hefei	0.04	0.04	0.75	0.07	0.09	Shenzhen	0.03	0.03	0.79	0.07	0.09
Changzhou	0.03	0.04	0.75	0.08	0.09	Chengdu	0.04	0.05	0.75	0.09	0.07
Shanghai	0.04	0.05	0.73	0.09	0.08	Chongqing	0.05	0.04	0.69	0.15	0.07
Nanjing	0.04	0.05	0.76	0.08	0.08	Guiyang	0.04	0.05	0.68	0.12	0.10
Suzhou	0.04	0.04	0.77	0.07	0.07	Kunming	0.02	0.05	0.76	0.09	0.08
Nanchang	0.04	0.04	0.74	0.09	0.09	Xi'an	0.04	0.06	0.74	0.10	0.06

latitude of city, and the precipitation is concentrated around 0. In the East China region, there is no significant relationship between maximum/minimum temperature/dressing index and latitude of city, the precipitation is concentrated around 0, and the wind speed is concentrated around 0.05. In Central China region, the maximum/minimum temperature increase as the latitude of decreases, the dressing index decreases as the latitude of city decreases, and the precipitation is concentrated around −0.07. In the South China region, the wind speed is concentrated around 0, the precipitation is concentrated around −0.04, and the locations with maximum temperature are generally higher than those with minimum temperature, indicating that the urban rail transit passenger volume in the South China region is more affected by maximum temperature. In the southwest region, there is no significant relationship between these five factors and the latitude of city, and the precipitation is concentrated around 0. In the northwest region, the locations with maximum temperature are higher than those with minimum temperature, indicating that the urban rail transit passenger volume in the northwest region is more affected by maximum temperature.

In general, the precipitation and wind speed in most cities are concentrated in a numerical range, indicating that the impact of precipitation and wind speed on urban rail transit passenger volume is consistent in such cities. The maximum/minimum temperatures show a positive correlation with the urban rail transit passenger volume in all cities. However, the relationship with latitude of city varies depending on the region. For example, in the North China region, there is a positive correlation with latitude of city, but in the East China region, there is a negative correlation with latitude of city, which also proves the climatic differences between different regions. The dressing index shows a negative correlation with urban rail transit passenger volume in all cities, and there is no changing pattern in its relationship with latitude of city.

5.4 Analysis and Evaluation on Decoupling

In this section, the relationship between meteorological comfort and urban rail transit passenger volume is studied, namely the relationship between the five meteorological factors as a whole and the urban rail transit passenger volume. Based on the calculation results, a classified heatmap is established, as shown in Fig. 4. According to statistics, the cities with the most Class A, Class B, and Class C days are Tianjin (24 days), Xiamen (188 days), and Hefei (205 days), respectively; the cities with the fewest are Changsha (6 days), Hefei (145 days), and Beijing (163 days).

With respect to the distribution pattern of Class A days in various cities, it is quite obvious that such days are mainly distributed on Mondays and the first day of work after holidays in Beijing, and on Fridays in Chongqing; the

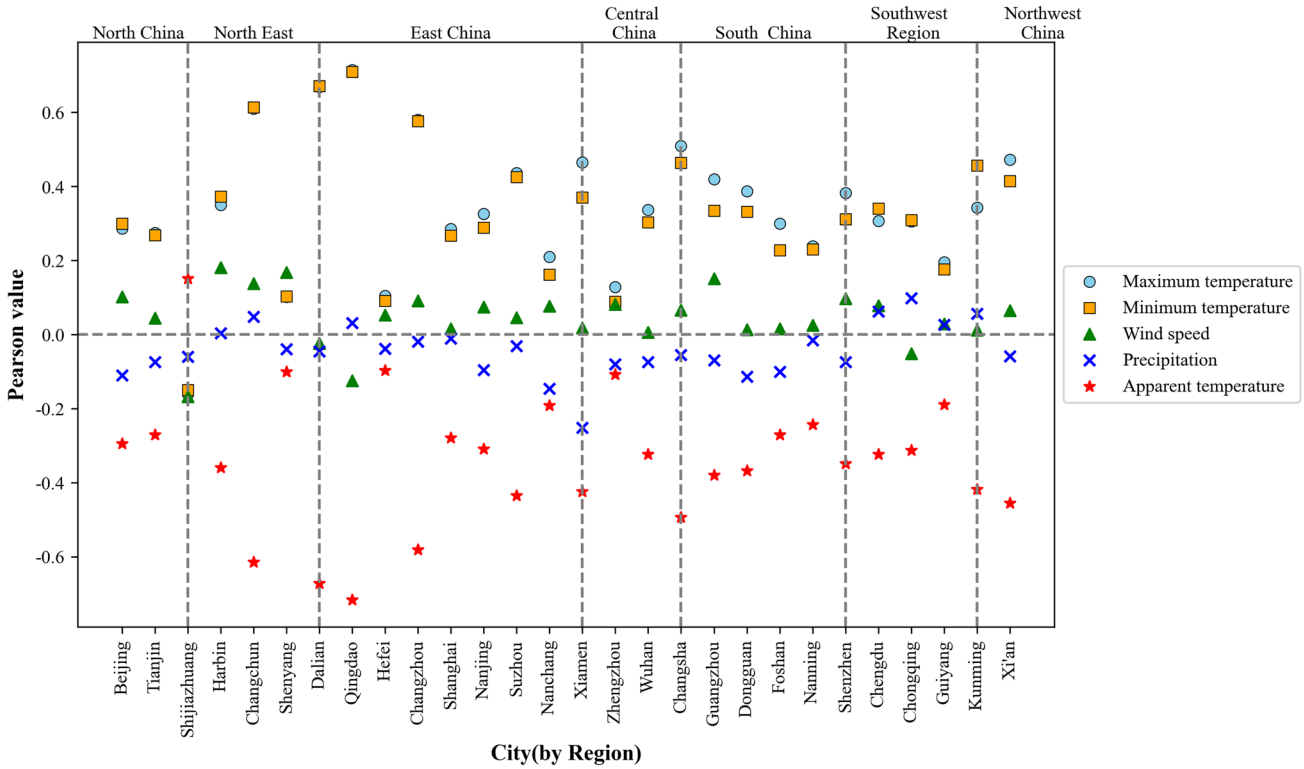

Fig. 3 Scatter plot of pearson correlation coefficient

regularity that appears in other cities is not very strong. Therefore, it is necessary to analyze the decoupling stability and further identify the relationship between meteorological factors and urban rail transit passenger volume. The analysis results of decoupling stability are shown in Table 11. Chongqing has the strongest decoupling stability. Eight Class A days occurred in Chongqing, of which 5 days are distributed on Mondays, with 1 day each on Spring Festival, Labor Day and Friday. Although Tianjin has the most Class A days, its decoupling stability is 5.50, not very high. Based on the daily distribution chart of meteorological comfort, the occurrence of extreme meteorological comfort in China is rare, as shown in Fig. 5. By observing the timing of Class A days occurring in Tianjin and Chongqing, it can be found that the reason why Chongqing is stable is because the meteorological comfort did not change significantly in the two consecutive days.

Similarly, comparing all cities, it can be found that, firstly, the number of Class A days occurring is not very high; secondly, the Class A days often occurred in the manner that the change in meteorological comfort was not significant in two consecutive days, and the meteorological environment on the second day deteriorated slightly as compared to the first day. In such case, the rapid increase in passenger volume seems to be more affected by the weekly travel patterns. After statistical analysis, the weekly patterns of Class A days are that they are highly likely to occur on Mondays in Beijing, Tianjin, Harbin, Changchun, Dalian, Qingdao, Hefei, Shanghai, Nanjing, Wuhan, Guangzhou, Shenzhen, Chengdu, Chongqing and Guiyang, are highly likely to occur on Fridays in Shijiazhuang, Shenyang, Changzhou, Suzhou, Nanchang, Xiamen, Zhengzhou, Changsha, Dongguan, Nanning, Kunming and Xi'an, and are highly likely to occur on Saturdays in Foshan. This may be due to the characteristics of urban travel. Those cities with Class A days occurring on Mondays are often the leading cities in their respective region, and perhaps Mondays are the beginning of a week of work; those cities with Class A days occurring on Fridays are often non-leading cities in a certain region, which may take on more travel from leading cities. In order to understand the relationship between them, the OD travel data within each region are required.

By adopting the measures to encourage travel, the urban rail transit passenger volume in Shijiazhuang was increased, but no Class A phenomenon occurs, which indicates that travel encouraging measures are effective for Shijiazhuang, but from a decoupling perspective, their effect is not obvious, and there is still potential to tap into passenger volume.

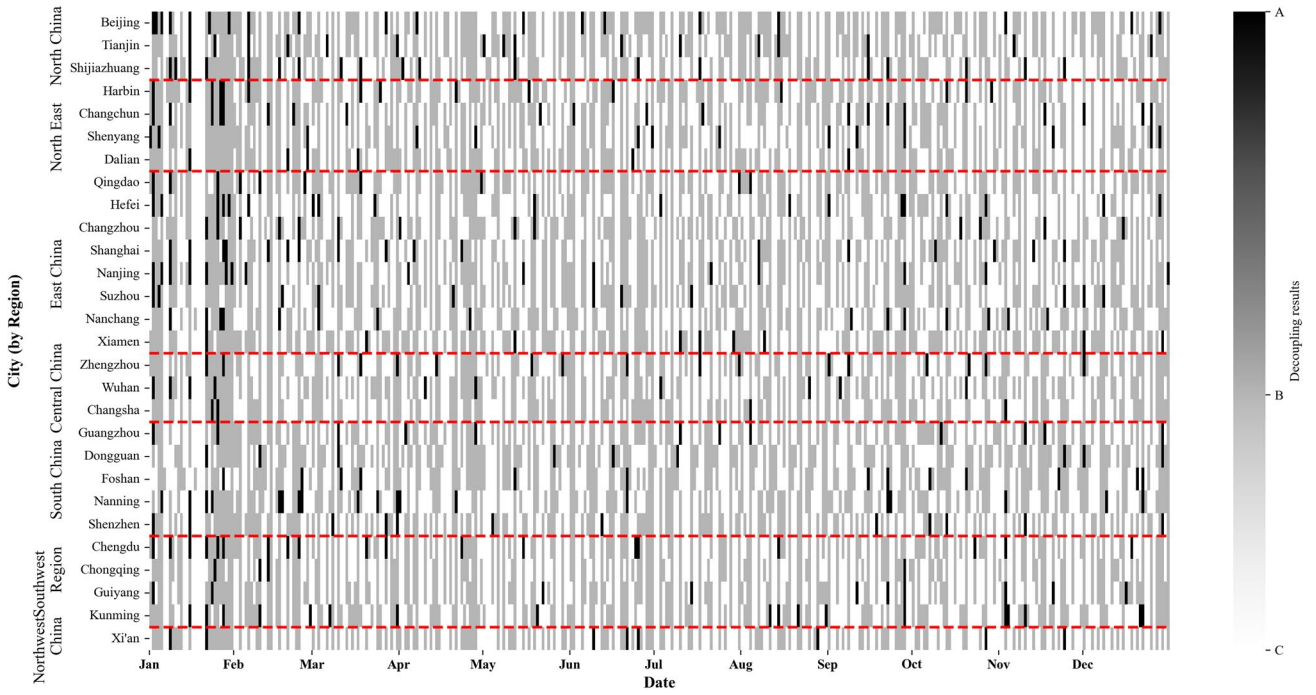

Fig. 4 Thermodynamic diagram of classification decoupling calculation results

Table 11 Stability of passenger volume decoupling in urban rail transit

City	Stability	Stability of average	City	Stability	Stability of average
Chongqing	0.90	364.78	Changchun	2.75	205.09
Suzhou	0.96	101.04	Guiyang	3.12	256.34
Wuhan	1.30	334.29	Beijing	3.32	227.73
Xi'an	1.32	91.64	Nanning	3.33	86.99
Qingdao	1.35	195.62	Shanghai	3.61	69.58
Changsha	1.44	100.03	Harbin	4.44	107.00
Xiamen	1.61	364.88	Nanjing	5.05	216.50
Hefei	1.69	39.19	Tianjin	5.50	584.39
Foshan	1.90	307.35	Changzhou	5.63	146.19
Guangzhou	2.14	195.93	Dongguan	6.00	202.95
Chengdu	2.20	167.78	Shijiazhuang	6.15	317.34
Zhengzhou	2.22	159.24	Shenyang	6.22	92.13
Kunming	2.4	479.61	Nanchang	6.40	487.27
Dalian	2.65	145.43	Shenzhen	7.92	315.22

5.5 Practical Implications and Policy Recommendations

Our findings have several implications for urban rail transit management and policy. First, the decoupling model provides a quantitative tool for identifying the extent to which ridership is resilient or vulnerable to meteorological fluctuations. Transportation authorities can use this information to anticipate passenger demand under adverse weather conditions and to adjust train frequencies, staffing, and emergency preparedness accordingly.

Second, the classification of decoupling states (Classes A, B, and C) offers a diagnostic framework. For example, cities frequently exhibiting Class C states may require investment in weather-resilient infrastructure, such as improved drainage systems, snow removal capacity, or enhanced station design to mitigate environmental impacts on passenger comfort.

Third, by monitoring the stability of decoupling over time, policymakers can evaluate whether interventions—such as improved passenger information systems, integrated weather alerts, or fare incentives during adverse weather—effectively enhance system robustness. This aligns with broader goals of sustainable urban mobility by ensuring service continuity and minimizing social disruption caused by weather events.

Finally, the model underscores the importance of incorporating meteorological comfort into transport planning alongside traditional built environment and demand-side factors. Policy recommendations include (1) integrating meteorological comfort indices into transport demand forecasting models, (2) strengthening cross-sector collaboration between meteorological agencies and transit authorities, and

Fig. 5 Daily distribution of meteorological comfort

(3) designing adaptive operational strategies that maintain ridership stability during environmental degradation.

6 Conclusions and Prospect

This study constructed a meteorological comfort model to analyze the decoupling relationship between meteorological comfort and urban rail transit ridership in 28 Chinese cities. By incorporating multiple meteorological factors—including maximum and minimum temperature, precipitation, wind speed, and dressing index—the model provides a multi-dimensional perspective for understanding how weather conditions shape daily transit demand.

The main findings can be summarized as follows:

(1) Heatmaps, combined with normalization, provide an effective tool to visualize daily passenger volume and meteorological comfort, allowing for intuitive recognition of travel patterns and stability across cities.
(2) Short-term travel encouraging measures, such as those observed in Shijiazhuang, can temporarily increase ridership, but show limited effect from a decoupling perspective, suggesting they are insufficient to fundamentally alter travel behavior.
(3) The relative weights of meteorological factors in the comfort index differ across regions, reflecting the heterogeneity of local climates.
(4) Individual meteorological factors have distinct impacts: maximum and minimum temperatures are positively correlated with ridership; dressing index shows a negative correlation; precipitation and wind speed exhibit region-dependent effects.
(5) The decoupling analysis reveals significant differences across cities. For instance, Tianjin recorded the highest number of Class A days (24 in 2023), though with unstable distribution, while Chongqing displayed greater stability, particularly on Mondays.

From a practical perspective, these results suggest that transportation authorities should integrate meteorological comfort indices into demand forecasting and service planning. The decoupling classification framework can help identify cities or periods with higher vulnerability, informing targeted strategies such as adaptive scheduling, enhanced weather-resilient infrastructure, and improved passenger information services during adverse conditions.

There are limitations to this study, as it focuses solely on rail transit ridership while excluding other public transport modes such as buses and trams. Future research could broaden the scope to multimodal systems, refine prediction algorithms with real-time meteorological data, and integrate operational scheduling data of rail vehicles. Comparative studies across different climatic regions or countries, using local meteorological standards, would also enhance the generalizability of the model. Such efforts will provide stronger guidance for improving urban resilience,

enhancing passenger services, and optimizing rail transit operation under changing meteorological conditions.

Author Contribution Zhanwei Cui was involved in conceptualization, methodology, software, resources, and writing—original draft. Yang Yang was responsible for conceptualization, methodology, formal analysis, validation, investigation, project administration, writing—reviewing and editing, funding acquisition, and data curation. Shengye Hu participated in validation and writing—reviewing and editing. Xin Liu performed data curation and visualization. Long Chen conducted visualization and investigation.

Funding This research was supported by funding from Fundamental Research Funds for the Central Universities (2024JBRC009) and National Natural Science Foundation of China (52572336).

Data Availability Data will be made available on request.

Declarations

Conflict of interest The authors declare that they have no known competing financial interests or personal relationships that could have appeared to influence the work reported in this paper.

References

1. Lin T, Srikukenthiran S, Miller E, Shalaby A (2018) Subway user behaviour when affected by incidents in Toronto (SUBWAIT) survey—a joint revealed preference and stated preference survey with a trip planner tool. Can J Civil Eng 45(8):623–633. https://doi.org/10.1139/cjce-2017-0442
2. Alam O, Kush A, Emami A et al (2021) Predicting irregularities in arrival times for transit buses with recurrent neural networks using GPS coordinates and weather data. J Ambient Intell Human Comput 12:7813–7826
3. Kim K (2020) Effects of weather and calendar events on mode-choice behaviors for public transportation. J Transp Eng Part A: Syst 146(7):04020056. https://doi.org/10.1061/JTEPBS.0000371
4. Shaaban K, Siam A (2021) Public transportation usage in a hot climate developing country. Transp Study Procedia 55:394–400. https://doi.org/10.1016/j.trpro.2021.07.002
5. Simon Lepage and Catherine Morency (2021) Impact of weather, activities, and service disruptions on transportation demand. Transp Study Rec 2675(1):294–304. https://doi.org/10.1177/0361198120966326
6. Yuldoshev Davron, Abdullaev Botir, Yusufkhonov Zokirkhon, Muminov Tulkin (2022) Determining the impact of weather indicators on passenger traffic in public transport. Universum: технические науки, 1-3(94):64-70
7. Ngo NS (2019) Urban bus ridership, income, and extreme weather events. Transp Res Part D Transp Environ 77:464–475. https://doi.org/10.1016/j.trd.2019.03.009
8. Chen Zhenhua, Wang Yuxuan (2019) Impacts of severe weather events on high-speed rail and aviation delays. Transp Res Part D: Transp Environ 69:168–183. https://doi.org/10.1016/j.trd.2019.01.030
9. He X (2022) Passenger flow organization of urban rail transit and passenger transport organization in emergencies. Transp Manager World 03:1–3
10. Geng K (2022) Fine control strategies for meteorological risks in shanghai's urban rail transit. Urban Mass Transit 25(03):86–90. https://doi.org/10.16037/j.1007-869x.2022.03.018
11. Keke Ji, Yang Qing, Ji Kaili, Zhang Shuting, Lin Chunwang, Li Zhengzhong (2024) Study on impact mechanism of abnormal passenger flow in urban rail transit. Railw Transp Econ, pp 1-11
12. Forero-Ortiz E, Martínez-Gomariz E, Cañas Porcuna M (2020) A review of flood impact assessment approaches for underground infrastructures in urban areas: a focus on transport systems. Hydrol Sci J 65(11):1943–1955. https://doi.org/10.1080/02626667.2020.1784424
13. Welch TF, Gehrke SR, Widita A (2018) Shared-use mobility competition: a trip-level analysis of taxi, bikeshare, and transit mode choice in Washington, DC. Transportmetrica A Transp Sci 16(1):43–55. https://doi.org/10.1080/23249935.2018.1523250
14 Yang B, Yang C, Ni L, Wang Y, Yao Y (2022) Investigation on thermal environment of subway stations in severe cold region of China: a case study in Harbin. Build Environ 212:108761
15. Jenkins K, Gilbey M, Hall J, Glenis V, Kilsby C (2014) Implications of climate change for thermal discomfort on underground railways. Transp Res Part D Transp Environ 30:1–9. https://doi.org/10.1016/j.trd.2014.05.002
16 Singhal Abhishek, Kamga Camille, Yazici Anil (2014) Impact of weather on urban transit ridership. Transp Study Part A Policy Practice. 69:379–391. https://doi.org/10.1016/j.tra.2014.09.008
17. Jain D, Singh S (2021) Adaptation of trips by metro rail users at two stations in extreme weather conditions: Delhi. Urban Climate 36:100766. https://doi.org/10.1016/j.uclim.2020.100766
18. Wang B (2023) Study on impact of different rainfall periods on passenger volume at subway stations. Western China Commun Sci Technol 09:147–150. https://doi.org/10.13282/j.cnki.wcst.2023.09.044
19. Lou Shurong (2016) Study on impact of rainy weather on passenger volume at urban rail transit stations by Lou Shurong. Southeast University
20. Li Rui (2018) Study on impact of rainfall on passenger volume at urban rail transit stations. Southeast University
21. Najafabadi S, Hamidi A, Allahviranloo M, Devineni N (2019) Does demand for subway ridership in Manhattan depend on the rainfall events? Transp Policy 74:201–213. https://doi.org/10.1016/j.tranpol.2018.11.019
22. Volovski M, Ieronymaki ES, Cao C, O'Loughlin JP (2021) Subway station dwell time prediction and user-induced delay. Transportmetrica A Transp Sci 17(4):521–539. https://doi.org/10.1080/23249935.2020.1798555
23. Huang Sheng (2022) Study on spatiotemporal pattern of impact on shanghai's subway commuting travel under rainfall scenarios by Huang Sheng [D]. Shanghai Normal University

24. Chen Jian; Luo Guohong (2024) Study on flood prevention plans and emergency measures for rail transit operations under extreme weather. Transp Manager World 03:10–12
25. Cui Jiayu, Liu Zhujuan (2023) Study on the influence of weather factors on urban rail transit passenger flow. TCSISR 1:169–181. https://doi.org/10.62051/311by728
26. Toto E, Rundensteiner EA, Li Y, Jordan R, Ishutkina M, Claypool K, Luo J, Zhang F (2016) PULSE: a real time system for crowd flow prediction at metropolitan subway stations. In: Berendt B et al. Machine learning and knowledge discovery in databases. ECML PKDD 2016. Lecture notes in computer science, vol 9853. Springer, Cham. https://doi.org/10.1007/978-3-319-46131-1_19
27. Li J (2018) Study on generation mechanism of residential rail transit travel under rainy and snowy weather by Li Junlong [D]. Southeast University
28 Wu J, Liao H (2020) Weather, travel mode choice, and impacts on subway ridership in Beijing. Transport Res Part A: Policy Practice 135:264–279
29. Sajan GV, Kumar P (2021) Forecasting and analysis of train delays and impact of weather data using machine learning. In:2021 12th international conference on computing communication and networking technologies (ICCCNT), Kharagpur, India, pp 1-8. https://doi.org/10.1109/ICCCNT51525.2021.9580176.
30. Manling Xu, Xiao Fu, Tang J et al (2020) Empirical study on impact of weather factors on urban subway passenger volume based on spatiotemporally-distributed intelligent transportation card data. Prog Geogr 39(01):45–55
31. Brazil W, White A, Nogal M, Caulfield B, O'Connor A, Morton C (2017) Weather and rail delays: analysis of metropolitan rail in Dublin. J Transp Geogr 59:69–76. https://doi.org/10.1016/j.jtrangeo.2017.01.008
32. Zhu Chengcheng (2018) Study on impact of rainy weather on rail commuter travel based on swipe card data by Zhu Chengcheng [D]. Southeast University
33. Xie Z, Peng B (2023) A framework for resilient city governance in response to sudden weather disasters: a perspective based on accident causation theories. Sustainability 15(3):2387. https://doi.org/10.3390/su15032387
34. Xiangguo Wu, Zhang Jiansong, Yiliang Hu, Bicheng Zhao, Gao Zhigang (2020) Discussion on time characteristics and influencing factors of rail transit passenger volume in Chongqing. Railw Transp Econ 42(11):117–122. https://doi.org/10.16668/j.cnki.issn.1003-1421.2020.11.20
35. Shumin Feng, Hao Liu, Laicheng Li (2022) Prediction model for rail transit passenger volume under rainy and snowy weather. J Harbin Inst Technol 54(09):1–6
36. Silva C, Martins F (2020) Traffic flow prediction using public transport and weather data: a medium sized city case study. In: Rocha Á, Adeli H, Reis L, Costanzo S, Orovic I, Moreira F (eds) Trends and innovations in information systems and technologies. WorldCIST 2020. Advances in intelligent systems and computing, vol 1160. Springer, Cham. https://doi.org/10.1007/978-3-030-45691-7_35
37. Fei J, Yan J, Chen J (2024) Study and application of ultra-short-term passenger volume prediction model for urban rail transit. Traffic Transp 40(01):47–52
38. Cui C, Jia H, Huang L, Zhang X (2016) Fuzzy multivariate NARX model for passenger entrance flow prediction in the Shanghai subway system. J Intell Fuzzy Syst 31:3047–3054. https://doi.org/10.3233/JIFS-169190
39. Wang J, Kong X, Zhao W, Tolba AM, Al-makhadmeh Z, Xia F (2018) STloyal: a spatio-temporal loyalty-based model for subway passenger flow prediction. IEEE Access 6:47461–47471
40 Wang J, Leng B, Wu J, Du H, Xiong Z (2020) Metroeye: a weather-aware system for real-time metro passenger flow prediction. IEEE Access 8:129813–129829
41. Xue F, Yao E, Huan N, Li B, Liu S (2020) Prediction of urban rail transit ridership under rainfall weather conditions. J Transp Eng Part A: Syst 146(7):04020061
42. He Y, Zhao Y, Tsui KL (2022) Short-term forecasting of origin-destination matrix in transit system via a deep learning approach. Transportmetrica A Transp Sci. https://doi.org/10.1080/23249935.2022.2033348
43. Fontes Tânia, Correia Ricardo, Ribeiro Joel, Borges José Luís (2020) A deep learning approach for predicting bus passenger demand based on weather conditions. Transp Telecommun 21(4):255–264
44. Sha S, Li J, Zhang Ke, Yang Z, Wei Z, Li X, Zhu X (2020) RNN-based subway passenger flow rolling prediction,. IEEE Access 8:15232–15240. https://doi.org/10.1109/ACCESS.2020.2964680
45. Izudheen S, Mulerikkal JP, John MJ, Malavika K, Joshy J, Beveira GM (2021) Short-term passenger count prediction for metro stations using LSTM network. Turk J Comp Math Educ 12(3):4026–4034
46. Yang Y, Huang HB, Li G et al (2025) A systematic review of resilience assessment and enhancement of urban integrated transportation networks[J]. J Transp Geogr 129:104420
47. Shuqing Li, Wei Li, Yaohong L, Bo Ma (2024) Short-term passenger volume prediction model for rail transit based on combinatorial deep learning. J Chongqing Jiaotong Univ (Natural Sci Ed) 43(02):92–99
48. Zheng J, Fang X, Wang C (2023) Method for predicting large passenger volume in urban rail transit based on time series decomposition. Urban Mass Transit 26(08):163–170. https://doi.org/10.16037/j.1007-869x.2023.08.031
49. Xiu C, Zhan S, Pan J, Peng Q, Lin Z, Wong SC (2024) Correlation-based feature selection and parallel spatiotemporal networks for efficient passenger flow forecasting in metro systems. Transportmetrica A: Transp Sci. https://doi.org/10.1080/23249935.2024.2335244
50. Nian G, Chen F, Li Z, Zhu Y, Sun D (2019) Evaluating the alignment of new metro line considering network vulnerability with passenger ridership. Transportmetrica A Transp Sci 15(2):1402–1418. https://doi.org/10.1080/23249935.2019.1599080
51. Faghih-Imani A, Eluru N (2016) Examining the impact of sample size in the analysis of bicycle-sharing systems. Transportmetrica A Transp Sci 13(2):139–161. https://doi.org/10.1080/23249935.2016.1223205
52. Lei Bin; Zhang Yuan; Hao Yarui; Jing Lizhu (2022) Study progress on short-term prediction of urban rail transit passenger volume. J Chang'an Univ (Natural Science Edition) 42(01):79–96. https://doi.org/10.19721/j.cnki.1671-8879.2022.01.005
53. Shen L, Long Y, Tian L et al (2023) The impact of built environment on the commuting distance of middle/low-income tenant workers in mega cities based on nonlinear analysis in machine learning. Urban Rail Transit 9:294–309. https://doi.org/10.1007/s40864-023-00202-4
54. Öztürk O, Bozkurtoğlu E (2023) Investigation of the effects of important factors in suburban rail route determination with MCDM. Urban Rail Transit 9:233–245. https://doi.org/10.1007/s40864-023-00200-6
55 Freitas C (1979) Human climates of northern China. Atmos Environ 13(1):71–77
56. Müller J, Hothorn T, Yuan Y, Seibold S, Mitesser O, Rothacher J, Menzel A (2024) Weather explains the decline and rise of insect biomass over 34 years. Nature 628(8007):349–354

57. Qi J, Chen B (2012) Decoupling analysis for urban industrial sectors. Chin Popul Resour Environ 22(08):102–106
58. Netek R, Pour T, Slezakova R (2018) Implementation of heat maps in geographical information system—exploratory study on traffic accident data. Open Geosci 10(1):367–384. https://doi.org/10.1515/geo-2018-0029
59. Gull SF, Skilling J (1984) Maximum entropy method in image processing[C]//Iee proceedings f (communications, radar and signal processing). IEE 131(6):646–659
60. Schober P, Boer C, Schwarte LA (2018) Correlation coefficients: appropriate use and interpretation. Anesth Analg 126(5):1763–1768